Mo-Doped Mesoporous Silica for Thiophene Hydrodesulfurization: Comparison of Materials and Methods

Adam C. Sorensen, Bethany L. Fuller, Andrew G. Eklund, and Christopher C. Landry*

Department of Chemistry, Cook Physical Science Building, University of Vermont, Burlington, Vermont 05405

Received February 21, 2003. Revised Manuscript Received February 9, 2004

The mesoporous silica APMS-30 was compared to MCM-41 and MCM-48 as a substrate for the hydrodesulfurization (HDS) of thiophene with H_2. Mo was introduced to these materials by four methods: dry impregnation of the calcined silica with MoO_3, wet impregnation with aqueous $(NH_4)_6Mo_7O_{24}\cdot 4H_2O$, "reactive" impregnation with $MoCl_3$ in toluene, or in situ addition of $(NH_4)_6Mo_7O_{24}\cdot 4H_2O$ to the reaction mixture (APMS-30 only). Mo loading was approximately 6 wt % (Si/Mo = 24). Samples were characterized by chemical analysis, XRD, N_2 physisorption, SEM, and TEM. All samples were active for HDS and showed decreasing catalytic performance as a function of time, generally leveling out at total thiophene conversions between 22.8% and 57.4% after 75 min. Mo−APMS-30 showed the highest conversions, although Mo−MCM-48 synthesized by dry impregnation had slightly higher total conversion. Product distributions showed a shift from more hydrogenated to less hydrogenated C_4 compounds as conversion decreased, and low amounts of C_1, C_2, and C_3, compounds indicated that hydrocarbon cracking did not occur to a significant degree. Surface area did not appear to be a significant factor in catalytic performance.

Introduction

Mesoporous silica has been studied in recent years for applications ranging from filtration to catalysis.[1−4] A variety of conditions can be used to produce mesoporous silica, but the most common process involves the polymerization of silica in basic aqueous solution. MCM-41 and MCM-48, with hexagonal and cubic pore structures, have been extensively studied.[5,6] Neutral[7] and acidic[8−15] aqueous conditions can also be used to prepare mesoporous materials. The synthesis of APMS-30 (acid-prepared mesoporous spheres, 30 Å pores),[2,16,17] which is similar to other spherical mesoporous silicas prepared elsewhere,[4,18−21] has recently been reported. In contrast to most other mesoporous silicas, the synthesis of APMS-30 is complete in less than 2 h. Combined with the rapid calcination technique based on microwave irradiation that has also been recently reported,[22] the completed, calcined, porous material can be prepared in an afternoon. The pore diameter and particle size of APMS-30 are also easily modified by changing the synthetic parameters. APMS-30 has been primarily used in chromatographic applications, since spherical particles do not pack together as densely as mesoporous materials with irregular particle morphologies.[2,3] The spherical particle morphology is also easily recognizable by microscopic techniques (for example, fluorescence and confocal microscopies).[23]

Several papers have described the preparation of mesoporous silica containing Mo. For the most part, the

* To whom correspondence should be addressed. E-mail: cclandry@zoo.uvm.edu. Internet: http://www.uvm.edu/~cclandry.

(1) Corma, A. *Chem. Rev.* **1997**, *97*, 2373.
(2) Gallis, K. W.; Araujo, J. T.; Duff, K. J.; Moore, J. G.; Landry, C. C. *Adv. Mater.* **1999**, *11*, 1452.
(3) Gallis, K. W.; Eklund, A. G.; Jull, S. T.; Araujo, J. T.; Moore, J. G.; Landry, C. C. *Stud. Surf. Sci. Catal.* **2000**, *129*, 747.
(4) Boissière, C.; Kümmel, M.; Persin, M.; Larbot, A.; Prouzet, E. *Adv. Func. Mater.* **2001**, *11*, 129.
(5) Kresge, C. T.; Leonowicz, M. E.; Roth, W. J.; Vartuli, J. C.; Beck, J. S. *Nature* **1992**, *359*, 710.
(6) Beck, J. S.; Vartuli, J. C.; Roth, W. J.; Leonowicz, M. E.; Kresge, C. T.; Schmitt, K. D.; Chu, C. T−W.; Olson, D. H.; Sheppard, E. W.; McCullen, S. B.; Higgins, J. B.; Schlenker, J. L. *J. Am. Chem. Soc.* **1992**, *114*, 10834.
(7) (a) Bagshaw, S. A.; Prouzet, E.; Pinnavaia, T. J. *Science* **1995**, *269*, 1242. (b) Tanev, P. T.; Pinnavaia, T. J. *Science* **1995**, *267*, 2068.
(8) Huo, Q.; Leon, R.; Petroff, P. M.; Stucky, G. D. *Science* **1995**, *268*, 1324.
(9) Huo, Q.; Margolese, D. I.; Ciesla, U.; Demuth, D. G.; Feng, P.; Gier, T. E.; Sieger, P.; Firouzi, A.; Chmelka, B. F.; Schüth, F.; Stucky, G. D. *Chem. Mater.* **1994**, *6*, 1176.
(10) Huo, Q.; Margolese, D. I.; Ciesla, U.; Feng, P.; Gier, T. E.; Sieger, P.; Leon, R.; Petroff, P. M.; Schüth, F.; Stucky, G. D. *Nature* **1994**, *368*, 317.
(11) Zhao, D.; Feng, J.; Huo, Q.; Melosh, N.; Frederickson, G. H.; Chmelka, B. F.; Stucky, G. D. *Science* **1998**, *279*, 548.
(12) Zhao, D.; Huo, Q.; Feng, J.; Chmelka, B. F.; Stucky, G. D. *J. Am. Chem. Soc.* **1998**, *120*, 6024.
(13) Luan, Z.; Hartmann, M.; Zhao, D.; Zhou, W.; Kevan, L. *Chem. Mater.* **1999**, *11*, 1621.
(14) Yang, H.; Coombs, N.; Ozin, G. A. *Nature* **1997**, *386*, 692.
(15) Ozin, G. A.; Yang, H.; Sokolov, I.; Coombs, N. *Adv. Mater.* **1997**, *9*, 662.
(16) Gallis, K. W., Ph.D. Thesis dissertation, University of Vermont, **2001**.
(17) Gallis, K. W.; Landry, C. C. U.S. Patent 6,334,988, 2002.
(18) Qi, L.; Ma, J.; Cheng, H.; Zhao, Z. *Chem. Mater.* **1998**, *10*, 1623.
(19) Schacht, S.; Huo, Q.; Vogt-Martin, I. G.; Stucky, G. D.; Schüth, F. *Science* **1996**, *273*, 768.
(20) Huo, Q.; Feng, J.; Schüth, F.; Stucky, G. D. *Chem. Mater.* **1997**, *9*, 14.
(21) Yang, H.; Vork, G.; Coombs, N.; Sokolov, I.; Ozin, G. A. *J. Mater. Chem.* **1998**, *8*, 743.
(22) Gallis, K. W.; Landry, C. C. *Adv. Mater.* **2001**, *13*, 23.

10.1021/cm030239p CCC: $27.50
Published on Web 05/01/2004

purpose of Mo incorporation is to use the resulting materials in catalytic applications. In particular, Mo species are useful in hydrodesulfurization (HDS), the catalytic removal of sulfur from organic species in the presence of H_2 and/or H_2S. Methods of producing Mo-doped mesoporous silicas have included the direct addition of a Mo source to the synthesis mixture,[24−27] grinding MoO_3 with silica followed by a heating step to disperse the Mo,[28,29] the application of solutions of molecular Mo species to mesoporous silica,[26,30−34] or other methods.[35−37] However, there has been no complete study of the relationship between the porosity of the silica (surface area, pore diameter, pore volume) and the catalytic properties of the Mo-doped silicas. In addition, there has been no comparison of these different methods in terms of the catalytic ability of the resultant materials. Our interest in using APMS-30 in a variety of applications has led us to investigate the relative effectiveness of several related Mo-doped materials for HDS. In this paper we report on the use of Mo-doped MCM-41, MCM-48, and APMS-30 in the HDS of thiophene.

Experimental Section

Materials and Methods. Powder X-ray diffraction (XRD) experiments were performed on a Scintag $\times 1$ $\theta-\theta$ diffractometer equipped with a Peltier (solid-state thermoelectrically cooled) detector using Cu Kα radiation. N_2 adsorption and desorption isotherms were obtained on a Micromeritics ASAP 2010 instrument. Samples were degassed at 200 °C under vacuum overnight prior to measurement. Surface areas were measured using the BET method, and pore size distributions were calculated from the BJH method. Scanning electron micrographs (SEM) were acquired using a JEOL JSM-T300 instrument operating at 20 kV. Samples were sputtered with gold to reduce charging. Transmission electron microscopy (TEM) was performed on either a JEOL 100S or JEOL 100CXZ instrument operating at 100 kV. Samples were prepared by mounting in epoxy resin and microtoming to obtain a thin slice. Chemical compositions were obtained by proton-induced X-ray emission (PIXE) by the Element Analysis Corp., Lexington, KY, and by Galbraith Laboratories, Knoxville, TN. Calcinations were carried out in a box furnace under conditions of flowing air. The following heating profile was used for calcinations: 2 °C/min ramp to 450 °C, 240 min hold at 450 °C, 10 °C/min ramp to 550 °C, 480 min hold at 550 °C. Heating of the quartz tube used for catalysis was performed with a high-temperature heating tape connected to a temperature controller (Dyna-Sense MKI) fitted with a thin film detector (Omega). An Agilent model 6890 gas chromatograph (GC) fitted with a GS-GASPRO column (J&W Scientific, 15 m × 0.32 cm) and a flame ionization detector (FID) was used to analyze HDS products. Product distributions were calculated by adjusting the FID peak areas with ECN values for each product.[38] Parr autoclaves were purchased from the Parr Instrument Corp. MoO_3 and $(NH_4)_6Mo_7O_{24}{\cdot}4H_2O$ were purchased from Fisher. $MoCl_3$, tetraethyoxysilane (TEOS, 98%), cetyltrimethylammonium bromide (CTAB), and thiophene (97%) were obtained from Aldrich and used as received. Gases (H_2, He, N_2) were obtained from Merriam-Graves. The synthesis of gemini surfactants with the general formula "$n-m-n$" has been previously reported.[39]

Synthesis of MCM-48. The gemini surfactant $[CH_3(CH_2)_{21}N^+(CH_3)_2(CH_2)_{12}N^+(CH_3)_2(CH_2)_{21}CH_3)]Br_2$ ("22−12−22", 4.46 g, 4.56 mmol) was added to 172.5 g of H_2O. NaOH (2 M, 23.4 g) was added, and the solution was stirred and heated to 60 °C. At this point the solution was slightly cloudy and off-white in color. After cooling the solution slightly, TEOS (15.0 g, 72.0 mmol) was added. The solution was stirred for 12 h, during which time an off-white solid precipitated. The solid was collected by filtration, washed, air-dried, and suspended in 500 mL of H_2O at 100 °C for 7 days. The off-white powder was then recollected by filtration, washed, dried, and calcined. As with all samples, the product was kept in a closed vial but was not explicitly protected from air.

Synthesis of MCM-41. CTAB (4.00 g, 11.0 mmol) was dissolved in a solution of 196 g of H_2O and NaOH (2 M, 25.0 g). TEOS (19.3 g, 92.4 mmol) was then added and the solution was stirred for 12 h. The resulting white powder was collected by filtration, washed, dried, and then suspended in 500 mL of H_2O at 100 °C for 7 days. The white powder was then recollected by filtration, washed, dried, and then calcined.

Synthesis of APMS-30. CTAB (1.20 g, 3.29 mmol) was added to 55.5 g of H_2O. Concentrated HCl (4.50 g) was added and the mixture was stirred until the CTAB was fully dissolved and the solution was clear. TEOS (5.65 g, 27.1 mmol) was then added and the mixture was stirred for 1 h. After about 30 min of stirring, the solution had become cloudy. The solution was then placed in a Parr autoclave and heated at 150 °C for 40 min. The autoclave was slowly cooled to room temperature and the resulting white powder was filtered, washed, dried, and then calcined.

Dry Impregnation. Molybdenum trioxide (0.100 g, 0.695 mmol, 0.695 mmol Mo) was placed in an agate mortar and finely ground with 1.0 g of mesoporous silica. The sample was then placed in a crucible in a furnace, heated at a rate of 1.5 °C/min to 450 °C, and held at that temperature for 10 h.

Wet Impregnation. Molybdenum heptamolybdate (0.115 g, 0.0988 mmol, 0.692 mmol of Mo) was dissolved in 10 mL of H_2O at room temperature and 1.0 g of mesoporous silica was added. The mixture was then stirred until the H_2O had evaporated (overnight). The resulting solid was then calcined by the same program used for dry impregnation.

"Reactive" Impregnation. In a drybox, $MoCl_3$ (0.140 g, 0.692 mmol, 0.692 mmol Mo) was added to 1.0 g of mesoporous silica in a Schlenk flask. The flask was capped with a rubber septum, removed from the drybox, and approximately 15 mL of dried, distilled toluene was added via syringe. The mixture was stirred and refluxed for 5 h. Following removal of the toluene via distillation, the sample was calcined by the same program as that used for dry impregnation.

(23) Moore, J. G. Ph.D. Thesis dissertation, University of Vermont, 2001.
(24) (a) Piquemal, J.-Y.; Manoli, J.-M.; Beunier, P.; Ensuque, A.; Tougne, P.; Legrand, A.-P.; Brégeault, J.-M. *Microporous Mesoporous Mater.* **1999**, *29*, 291. (b) Piquemal, J.-Y.; Briot, E.; Vennat, M.; Brégnault, J.-M.; Chottard, G.; Manoli, J.-M. *Chem. Commun.* **1999**, 1195.
(25) Jianwei, G.; Lefu, W.; Zhongtao, H.; Yingde, C. *Chin. J. Catal.* **2000**, *21*, 20.
(26) (a) Dai, L.-X.; Teng, Y.-H.; Tabata, K.; Suzuki, E.; Tatsumi, T. *Microporous Mesoporous Mater.* **2001**, *44−45*, 573. (b) Dai, L.-X.; Teng, Y.-H.; Tabata, K.; Suzuki, E.; Tatsumi, T. *Chem. Lett.* **2000**, 794.
(27) Che, S.; Sakamoto, Y.; Yoshitake, H.; Terasaki, O.; Tatsumi, T. *J. Phys. Chem. B* **2001**, *105*, 10565.
(28) Xie, Y. C.; Tang, Y. Q. *Adv. Catal.* **1990**, *37*, 1.
(29) (a) Cui, J.; Yue, Y.; Sun, Y.; Dong, W.-Y.; Gao, Z. *Chem. Res. Chin. University* **1998**, *14*, 284. (b) Yue, Y.; Sun, Y.; Gao, Z. *Catal. Lett.* **1997**, *47*, 167.
(30) Klimova, T.; Rodríguez, E.; Martínez, M.; Ramírez, J. *Microporous Mesoporous Mater.* **2001**, *44−45*, 357.
(31) Ferreira, P.; Gonçalves, I. S.; Kühn, F. E.; Lopes, A. D.; Martins, M. A.; Pillinger, M.; Pina, A.; Rocha, J.; Romão, C. C.; Santos, A. M.; Santos, T. M.; Valente, A. A. *Eur. J. Inorg. Chem.* **2000**, 2263.
(32) Chiranjeevi, T.; Kumar, P.; Rana, M. S.; Dhar, G. M.; Rao, T. S. R. P. *J. Mol. Catal. A* **2002**, *181*, 109.
(33) Ookoshi, T.; Onaka, M. *Chem. Commun.* **1998**, 2399.
(34) Song, C.; Reddy, K. M. *Appl. Catal. A* **1999**, *176*, 1.
(35) Morey, M. S.; Bryan, J. D.; Schwarz, S.; Stucky, G. D. *Chem. Mater.* **2000**, *12*, 3435.
(36) Kang, K. K.; Ahn, W. S. *J. Mol. Catal. A* **2000**, *159*, 403.
(37) Landau, M. V.; Vradman, L.; Herskowitz, M.; Koltypin, Y.; Gedanken, A. *J. Catal.* **2001**, *201*, 22.
(38) Sevcík, J. *Journal of Chromatography Library. Volume 4: Detectors in Gas Chromatography*; Elsevier: New York, 1976.
(39) Huo, Q.; Margolese, D. I.; Stucky, G. D. *Chem. Mater.* **1996**, *8*, 1147.

Scheme 1. Diagram of Catalysis Setup Used in HDS Tests[a]

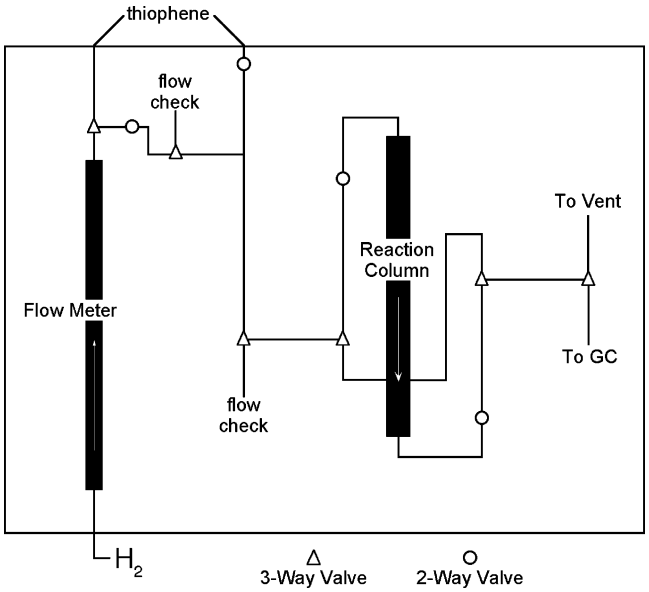

[a] A three-way valve at the top of the gas flow meter allowed manual switching between pure H_2 and thiophene-saturated H_2.

In Situ Addition of $(NH_4)_6Mo_7O_{24}\cdot 4H_2O$ to the APMS-30 Synthesis. The synthesis procedure was identical to the one used to prepare APMS-30, except that $(NH_4)_6Mo_7O_{24}\cdot 4H_2O$ (0.1 g, 0.0859 mmol, 0.601 mmol Mo) was added to the synthesis mixture prior to the addition of TEOS. Additionally, the resulting white product was not washed after filtration. The material was calcined using the standard procedure.

Hydrodesulfurization. Mo-doped mesoporous silica was pressed into a pellet and then cut into small pieces with a razor. A small amount of the pieces (0.50 g) were then collected and placed in a quartz reaction tube (see Scheme 1 for a schematic of the catalytic equipment). H_2 was then passed through the catalyst as it was heated to 400 °C (ramp = 13 °C/min) with heating tape wrapped around the quartz tube in the vicinity of the catalyst. The catalyst was then allowed to equilibrate for at least 1 h; after this time, the H_2 was passed through a saturator containing thiophene and then fed over the catalyst for 5 min with a flow rate of 27 mL/min. The flow was then switched back to pure H_2 while the effluent was analyzed by GC. After 40 min, the H_2 was switched back to the thiophene saturator for a 10 min feed. The procedure above was repeated for 15 and 60 min feeds. Corresponding total times on-stream for the catalyst were 5, 15, 30, and 75 min, with 40 min off-stream between each run. Thiophene conversion was determined from relative peak areas of products in the GC.

Results and Discussion

A total of nine samples were prepared by combining the three types of materials with the three methods of Mo impregnation (D = dry impregnation, W = wet impregnation, R = reactive impregnation). The 10th sample was prepared by in situ introduction of $(NH_4)_6Mo_7O_{24}\cdot 4H_2O$ directly into the APMS-30 synthesis mixture (designated I, in situ). The amount of Mo loading in all samples was 10 wt % MoO_3, which corresponded to 6.1 wt % Mo and a Si/Mo molar ratio of 24. Chemical analysis confirmed that this ratio remained essentially unchanged after calcination, catalysis, and catalyst regeneration. Mo species exist as oxoanions in most aqueous solutions, from acidic to basic pH. It is thought that the negatively charged silicate species present during the formation of MCM-41 and -48 in basic solution repel the Mo oxoanions, preventing their incorporation into the inorganic framework.[26,27] Our attempts to prepare Mo-doped MCM-41 and -48 through the direct addition of $(NH_4)_6Mo_7O_{24}\cdot 4H_2O$ to these reaction mixtures produced materials with extremely low concentrations of Mo, confirming the literature results. Since so much more Mo could be included by other methods, these materials were not used in our studies. However, the cationic species present during the formation of mesoporous silica in acidic solution allowed the preparation of Mo-doped APMS-30 by the in situ method at Si/Mo ratios that were comparable to the ratios produced by the other three methods.

N_2 Physisorption. Physical data from N_2 physisorption experiments are summarized in Table 1 and Figure 1. Following calcination and impregnation with Mo, all samples showed the large surface areas and narrow pore size distributions characteristic of mesoporous materials. The pore diameters of siliceous and Mo-doped MCM-48 were all larger than those of the other materials, which is likely due to the surfactant used to prepare MCM-48. This surfactant, "22−12−22", contains two C_{22} alkyl tails, in contrast to the single C_{16} alkyl tail of the surfactant used to prepare the other phases. The longer tails are responsible for the larger pores of the MCM-48 phases. Prior to Mo impregnation, MCM-48 also had the largest surface area and pore volume of the three phases. However, it showed the most severe changes upon impregnation, with the surface area and pore volume in one case (W-48) decreasing by more than 50%. This indicates that there was a substantial amount of pore collapse during all three impregnation techniques. MCM-41 showed smaller decreases in surface area upon impregnation than MCM-48, while APMS-30 showed the smallest changes. Pore volume decreases were similar for all three materials. This indicates that these two phases are more stable to postsynthetic treatments than MCM-48 prepared with gemini surfactants. The smaller decreases in surface area for APMS-30 materials are somewhat surprising given that it was prepared in a short time while MCM-41 and -48 were suspended at pH 7 and 100 °C for 1 week in order to increase the degree of polymerization of their inorganic frameworks. However, mesoporous silica prepared in acidic solution typically has a higher degree of polymerization than silica prepared in basic solution.[11,12,40] The APMS-30 material prepared by addition of the Mo source directly to the synthesis mixture (I-30) showed nearly identical surface area, pore volume, and pore diameter to the pure silica material, indicating that this method avoids the decreases in porosity associated with postsynthetic impregnation techniques.

Pore volumes for APMS-30 materials were substantially smaller than those for the other materials, which is a reflection of a more disordered pore structure. Pore diameters for MCM-41 and APMS-30 materials were similar, as expected for materials prepared with the same surfactant. As expected for a material with a higher degree of polymerization, there was no change in pore diameter upon Mo impregnation into APMS-30,

(40) Brinker, C. J.; Scherrer, G. W. *Sol−Gel Science: The Physics and Chemistry of Sol−Gel Processing*; Academic Press: Boston, 1990.

Table 1. Physical Data for Undoped and Mo-Doped Mesoporous Silicas[a]

sample	SA_{BET} (m^2/g)	ΔSA_{BET} (m^2/g)	ΣV_p (mL/g)	$\Delta\Sigma V_p$ (mL/g)	$pore_{BJH}$ (Å)	$\Delta pore_{BJH}$ (Å)	a_{cell} (Å)	Δa_{cell} (Å)
MCM-48	1265		1.40		32		99	
D-48	729	−526	0.85	−0.55	36	+4	105	+6
R-48	811	−454	0.95	−0.45	34	+2	93	−6
W-48	596	−669	0.52	−0.88	30	−2	96	−3
MCM-41	1189		0.95		25		45	
D-41	976	−213	0.89	−0.06	29	+4	43	−2
R-41	1019	−170	0.79	−0.16	26	+1	42	−3
W-41	989	−200	0.51	−0.44	25	0	38	−7
APMS-30	1125		0.53		24			
D-30	996	−129	0.46	−0.07	24	0		
R-30	1070	−55	0.41	−0.12	24	0		
W-30	738	−387	0.19	−0.34	24	0		
I-30	1094		0.52		25			
D-48-ac	729		0.87		36		104	
D-48-ac-r	754		0.87		35		104	
R-30-ac	989		0.37		24			

[a] Undoped materials are at the top of each group (except the last group). The number indicates the type of phase, corresponding to the undoped material. Prefixes: D, dry impregnation; R, reactive impregnation; W, wet impregnation; I, in situ addition to reaction mixture. Suffixes: ac, after catalysis; ac-r, after catalysis, regenerated. The unit cell parameters for MCM-48 and MCM-41 materials were calculated from the most intense peak in each pattern, assuming the *Ia*3*d* space group and *P*6*mm* plane group, respectively. APMS-30 has a disordered structure, preventing calculation of the unit cell parameter. Changes in each value (ΔSA, etc.) were determined after each postsynthetic process.

regardless of the method used. Interestingly, the dry and reactive impregnation methods caused increases in the pore diameters of MCM-48 and -41. Finally, analysis of samples after catalysis (D-48-ac, R-30-ac) and subsequent regeneration (D-48-ac-r) showed that the porosity of the impregnated materials did not change substantially after the initial Mo impregnation step. This is important in using the material in catalytic applications.

A comparison of materials produced by the three impregnation methods showed that, based on the severity of surface area and pore volume decreases, the wet impregnation method was the least favorable, since it generally caused the most pore collapse. In particular, the pore volumes decreased significantly upon wet impregnation. However, simply stirring the MCM-41 in the same amount of water *without* $(NH_4)_6Mo_7O_{24}$ and evaporating to dryness caused a significant decrease in surface area (757 m^2/g versus 1255 m^2/g) and pore volume (0.20 cm^3/g versus 1.00 cm^3/g). This suggests that the wet impregnation method, which is the most commonly used in the literature references, is the least effective in terms of retention of the desired porosity characteristics of mesoporous silica.

Powder X-ray Diffraction (XRD). XRD spectra for Mo-impregnated materials are shown in Figure 2. In general, MCM-41 and -48 showed some decrease in ordering, as determined by the decrease in intensities and increase in peak widths. Since APMS-30 showed only a single diffraction peak, changes in ordering for this material are more difficult to determine by XRD. Based on these changes, wet impregnation caused the most significant loss of order, confirming the results from the N_2 physisorption experiments described above. Materials prepared by dry impregnation retained the most ordering, with the reactive method giving intermediate results. It appears from these data that solution-based impregnation treatments caused more disruption of the porous framework than the dry impregnation method.

Although others have noted that heating ammonium heptamolybdate to temperatures above 700 K produces MoO_3,[41] no MoO_3 peaks appeared in the XRD patterns for the dry impregnation samples following the heating step, implying that the MoO_3 had been well-dispersed into the framework or that larger MoO_3 particles had been broken down into much smaller particles that were not observable by XRD. In the other methods of Mo introduction, mixtures of Mo sources in solvents were dried onto the porous silica samples, which were also subsequently calcined in air at 450 °C. These samples also did not show any XRD peaks other than those at low angles due to the mesoporous silica. This indicates that the Mo in all samples, regardless of the method of preparation, has been dispersed throughout the porous silica substrates. Similarly, XRD spectra of I-30 showed that no peaks for any Mo species were present either immediately following synthesis or after calcination.

A comparison of XRD spectra for MCM-48, D-48, D-48-ac (after catalysis), and D-48-ac-r (after catalysis and regeneration) showed that successive postsynthetic treatments caused increasing amounts of disruption in the pore structure (Figure 3). Decreases in peak intensity following impregnation, catalysis, and regeneration were observed for all samples. However, N_2 physisorption data (Table 1) indicated that the porosity of the D-48 samples remained fairly constant after the initial Mo impregnation. The combination of XRD and physisorption data indicate that although the individual pore ordering lengths (i.e. grains) within the sample decrease upon catalysis and regeneration, the pore structure remains intact.

Sample D-48-ac showed several very small peaks at higher angles (above 20°) following catalysis. These peaks were only apparent upon expansion of the XRD pattern (Figure 4). A comparison of the XRD spectra of MoO_3, MoS_2, and D-48-ac showed that the peaks in the

(41) Wienold, J.; Jentoft, R. E.; Ressler, T. *Eur. J. Inorg. Chem.* **2003**, *6*, 1058.

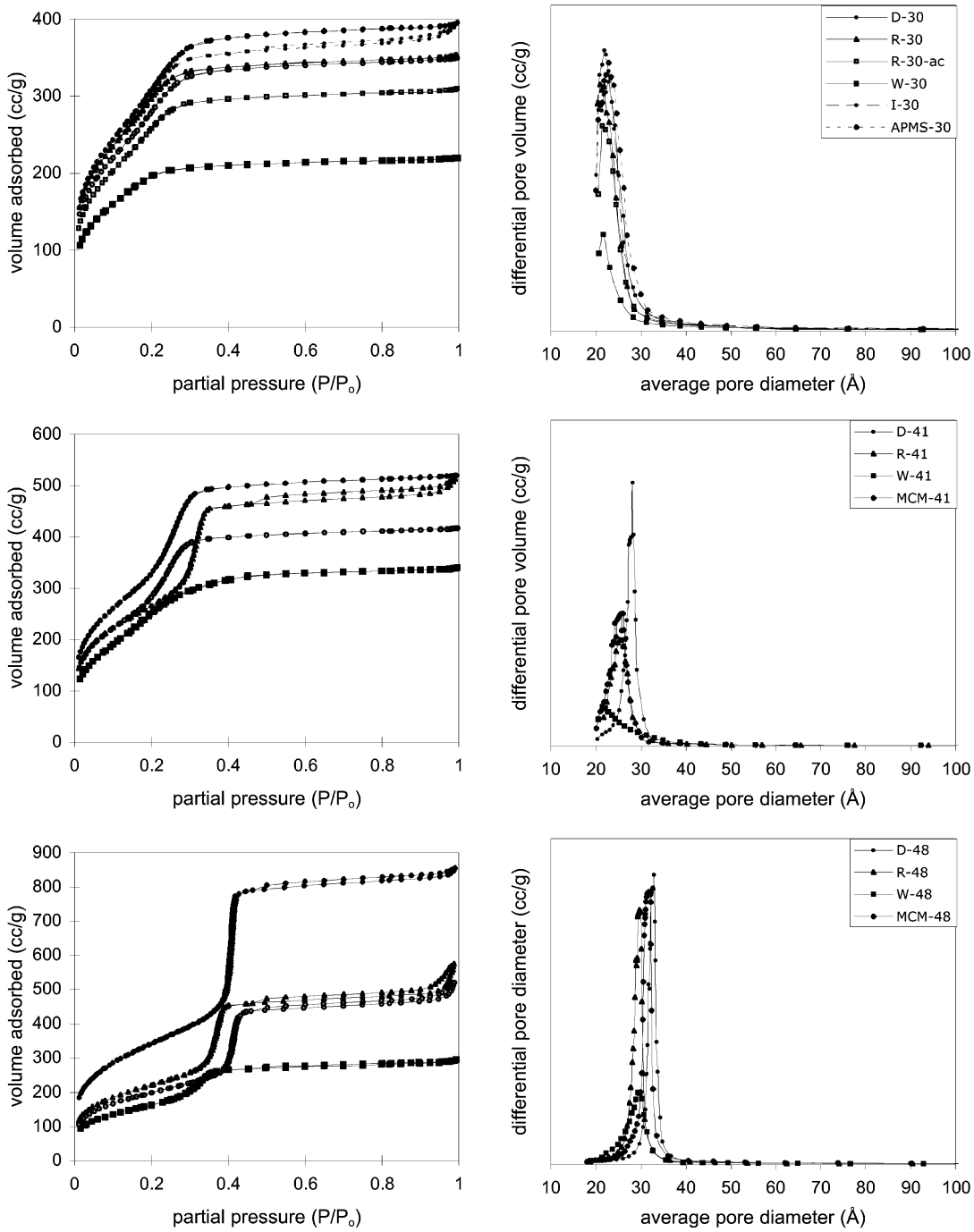

Figure 1. N_2 physisorption isotherms for Mo-doped silicas: top, Mo−MCM-48; middle, Mo−MCM-41; bottom, Mo-APMS-30.

D-48-ac spectrum at 26° and 37° are not due to the formation of these Mo species. The disappearance of these peaks upon regeneration in air (D-48-ac-r) indicates that these peaks may be due to carbon deposits remaining in this sample after catalysis. While the dry-impregnated samples were more ordered than other Mo-impregnated samples, the materials varied widely in properties from sample to sample (D-48 vs D-41 and D-30).

Electron Microscopy. TEM images of I-30 and I-30-ac were typical of what was observed for all materials prior to catalysis, namely, the lack of any noticeable large clusters of Mo. This was consistent with XRD spectra, which only showed peaks due to mesoporous ordering. The image of I-30-ac showed that even after catalysis and partial sulfidation, large Mo-containing particles were absent. However, there were some very small discrete particles that were apparently too small to be detected by XRD. This was consistent with STEM elemental maps on similar samples, which showed some slight but noticeable variation in Si/Mo ratio.[27] An SEM image of I-30 (Figure 5) showed the spherical particle morphology expected for APMS-30;[2] the addition of $(NH_4)_6Mo_7O_{24}$ to the synthesis mixture did not appear to alter the formation of this particle morphology.

Catalysis. HDS was performed in a catalysis rig (Scheme 1) by flowing an H_2/thiophene mixture over a pelletized sample of Mo-doped mesoporous silica at 400 °C. The substrate was pretreated in flowing H_2 prior to catalysis, and sequential HDS runs were performed to determine the change in thiophene conversion and product distributions over time. Table 2 shows the total

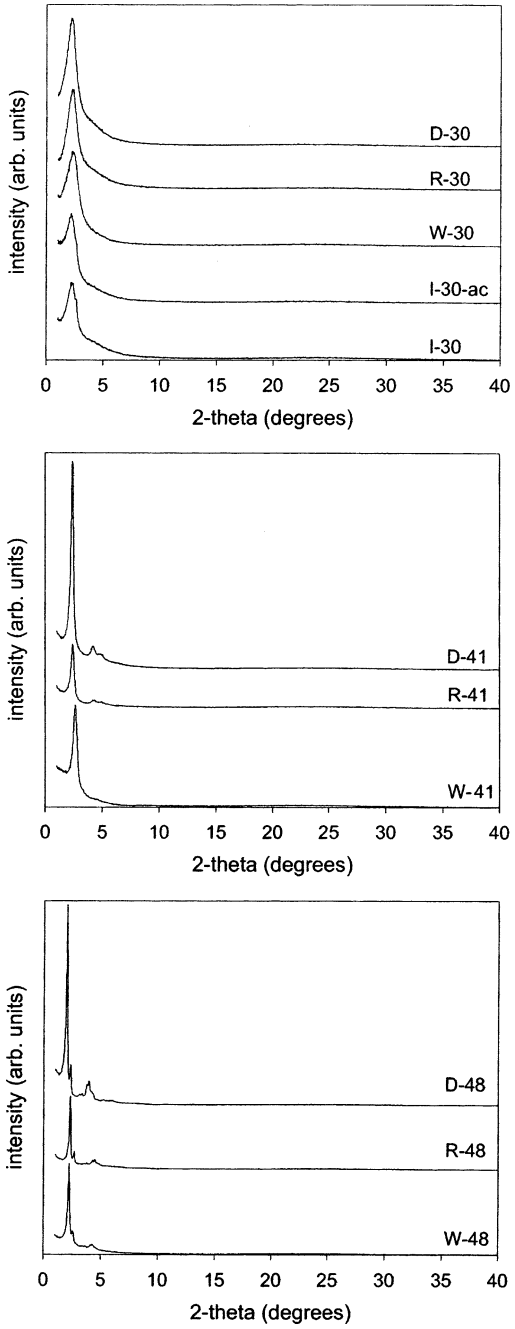

Figure 2. Powder XRD patterns of Mo-doped silicas: top, Mo−APMS-30; middle, Mo−MCM-41; bottom, Mo-MCM-48.

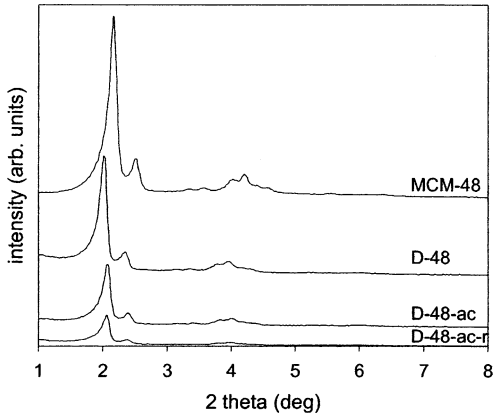

Figure 3. Powder XRD patterns of undoped and Mo-doped MCM-48 upon successive post-treatments: D-48, Mo-doped MCM-48 before HDS catalysis; D-48-ac, the same sample after catalysis; D-48-ac-r, the same sample after catalysis and regeneration by calcination.

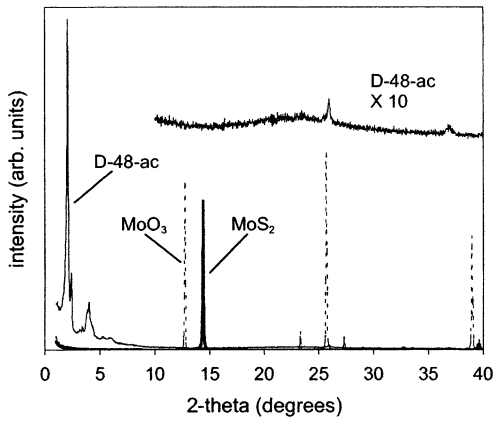

Figure 4. Powder XRD patterns of D-48-ac (solid), MoO_3 (dashed), and MoS_2 (bold).

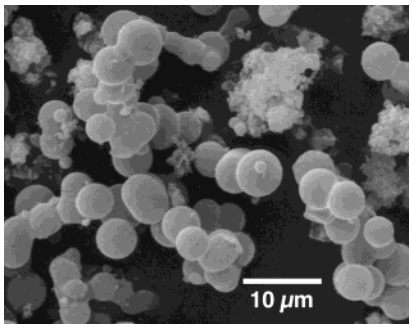

Figure 5. SEM of I-30.

conversion of thiophene and the product distributions for the 10 samples, at the shortest (5 min) and longest (75 min) reaction times. Catalytic activities of the Mo-doped materials, scaled to the amount of Mo present, are summarized in Figure 6. Control experiments performed with undoped silica showed no conversion of thiophene. All samples were active for HDS, particularly at short reaction times. After 5 min, some samples showed approximately 98% conversion of thiophene. Over time, total conversion decreased significantly, reaching values of approximately 20−50%. It is interesting to note that the sample prepared by the in situ addition of $(NH_4)_6Mo_7O_{24}$ showed the highest residual conversion (57.4%) after this time. This indicates either the presence of more active Mo sites, more exposed Mo, or both. The product distribution is also significant. C_3 or smaller organic fragments comprised only a small amount of the total product distribution, regardless of reaction time, indicating that hydrocarbon cracking was not an important pathway during HDS performed by this method. Of the C_4 products, butane formed the largest component at short reaction times and was a major component even at longer reaction times. Samples with low conversions of thiophene also showed higher amounts of monoalkenes, with *trans*-2-butene as the major or second most prevalent component. For example, the amount of *trans*-2-butene generally doubled over the reaction times studied in these experiments. These results indicate that hydrogenation was an important secondary process, particularly for catalysts that were more active. Although several papers have noted 1,3-butadiene as a major product, it was present

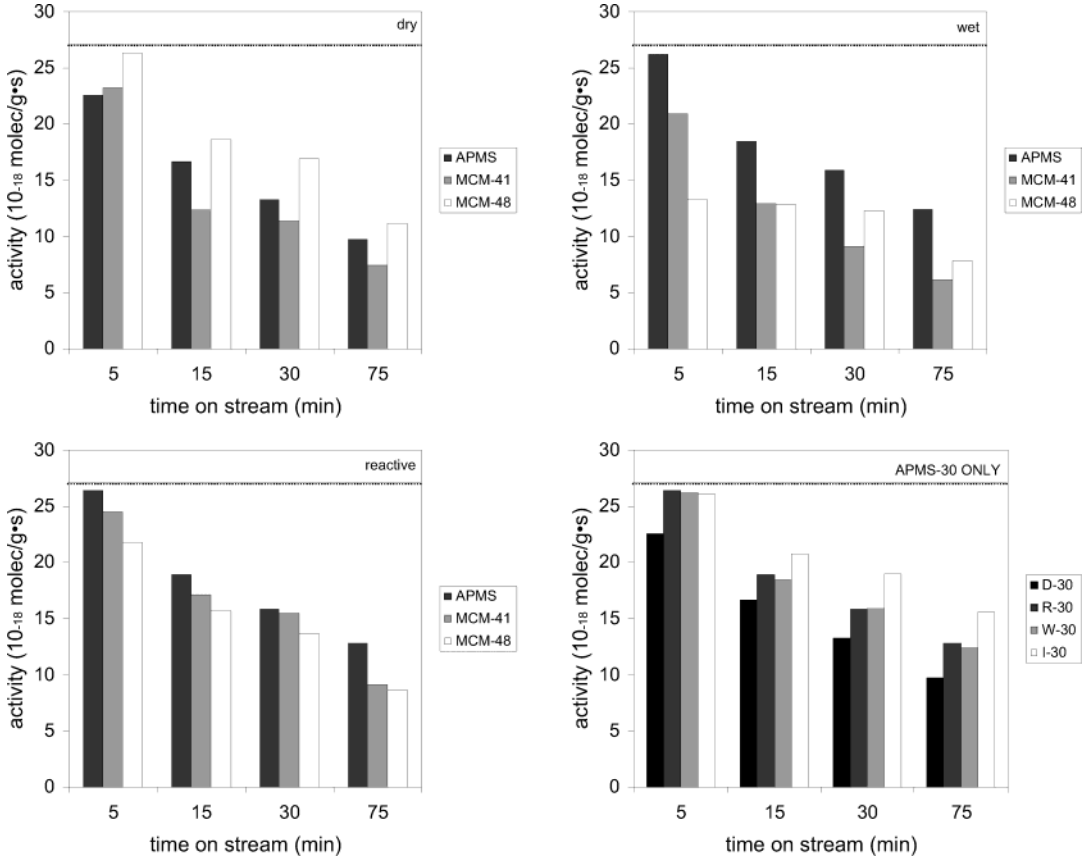

Figure 6. Catalyst activities, grouped according to method of impregnation and plotted with time on the horizontal axis. The graph on the right at the bottom contains activities of APMS-30 samples only. Activity was calculated as $(0.6[\text{thiophene}]FN_Ac)/(10^{18}g_{Mo})$, where [thiophene] = concentration of thiophene in mol/mL, F = flow rate in mL/min, N_A = Avogadro's number, c = percent conversion of thiophene, and g_{Mo} = total mass of Mo in the catalyst. The units of molecules/g•s refer to the number of thiophene molecules converted per second, normalized to the mass of Mo. The dashed horizontal line in each graph represents the maximum possible activity based on 100% conversion of thiophene.

Table 2. Product Distribution and Total Conversion from HDS of Thiophene by Mo-Doped Mesoporous Silicas at Selected Reaction Times[a]

sample	total % conversion	1,3-butadiene (wt %)	*trans*-2-butene (wt %)	*cis*-2-butene (wt %)	1-butene (wt %)	butane (wt %)	$C_1 - C_3$ (wt %)
			Time on Stream = 5 min				
D-48	97.2	0.890	11.7	8.28	6.50	*63.6*	8.99
R-48	80.4	0.813	18.6	13.1	10.1	*51.2*	6.10
W-48	49.0	1.90	*30.2*	21.2	16.9	18.1	11.9
D-41	85.7	3.29	20.8	14.4	10.5	*43.9*	7.20
R-41	90.4	0.732	15.3	10.7	8.13	*57.4*	7.59
W-41	77.3	0.451	13.9	9.63	7.69	*50.2*	18.0
D-30	83.2	8.00	24.6	17.4	13.7	*28.0*	8.23
R-30	97.4	1.35	13.2	9.21	7.05	*56.9*	12.2
W-30	96.8	1.07	13.4	9.42	7.42	*58.2*	10.5
I-30	96.3	2.20	14.9	10.5	8.43	*46.5*	17.5
			Time on Stream = 75 min				
D-48	41.3	1.42	24.2	17.1	13.4	*36.0*	7.58
R-48	32.0	1.53	26.7	18.8	14.3	*32.1*	6.23
W-48	29.0	1.40	*29.7*	21.0	16.9	25.0	6.49
D-41	27.4	1.19	*31.1*	21.7	15.8	26.2	4.13
R-41	33.6	1.72	25.1	17.9	13.5	*34.3*	7.21
W-41	22.8	1.04	*32.1*	22.4	17.4	17.7	9.59
D-30	36.0	1.61	*31.1*	21.9	17.4	19.5	8.76
R-30	47.3	1.79	26.2	18.5	14.1	*30.0*	9.35
W-30	45.8	2.02	*28.1*	20.0	15.6	24.5	9.75
I-30	57.4	2.27	23.6	16.9	13.3	*33.0*	11.0

[a] Italic numbers indicate the product present in the largest amount. Percentages of each product were determined from GC data by scaling FID peak areas with ECN values taken from ref 38.

in very small amounts in our experiments and its concentration did not increase with reaction time. The HDS and hydrogenation mechanisms involved here appear to yield singly unsaturated C_4 products. As has

Table 3. Elemental Analysis Data for Mo-Doped Samples after Catalysis

sample	Si (wt %)	Mo (wt %)	S (wt %)	Si/Mo/S (mol ratio)
D-48-ac	41.6	6.40	2.45	22.2/1.0/1.2
R-48-ac	41.4	5.89	2.83	23.9/1.0/1.4
W-48-ac	41.6	4.67	2.19	30.4/1.0/1.4
D-41-ac	37.9	5.42	2.68	26.7/1.0/1.4
R-41-ac	33.9	5.81	3.04	22.3/1.0/1.6
W-41-ac	41.2	4.69	1.22	30.1/1.0/0.8
D-30-ac	35.2	5.48	1.82	24.6/1.0/1.0
R-30-ac	35.2	5.35	2.21	25.2/1.0/1.2
W-30-ac	36.4	5.92	2.30	23.5/1.0/1.2
I-30-ac	32.7	4.87	2.35	25.7/1.0/1.4

been reported previously, Mo catalysts without promoter metals such as Co or Ni tend to show high levels of hydrogenated products while Co− or Ni−Mo show higher levels of unsaturated products.[42,43] In each case, the total conversion of thiophene can be high, indicating that although hydrogenation varies with the presence of promoter metals, HDS does not. It is also interesting to note that the ratio of *trans*-2-butene to *cis*-2-butene was the same regardless of reaction time or the type of substrate. The ratio (approximately 60/40) is what would be expected from a thermodynamic mixture of the two butenes in the presence of a hydrogenation source.[44] This leads to the conclusion that the HDS mechanism is similar to that indicated by Suslick et al., in which initial homolytic cleavage of the thiophene C−S bond and hydrogenolysis to give H_2S and butadiene was followed by rapid hydrogenation to 1-butene. This product either underwent slow hydrogenation to butane or was isomerized to a thermodynamic mixture of butenes.[42,45]

In general, product distributions did not show significant changes after 30 min of reaction time, while conversions continued to decrease. This indicated that the initial 30 min of reaction time were important in establishing the activity of the catalyst. It is likely that some sulfidation of Mo occurred during this time, since H_2S was produced during HDS. Chemical analysis of substrates after catalysis (Table 3) showed sulfur contents of 0.8−2.8 wt %, with Mo/S molar ratios of 0.6−1.6. The species present were likely either a mixture of MoO_3 and MoS_2 or a mixed Mo oxide−sulfide with partially reduced Mo. The sulfur could be removed by calcination in air to regenerate MoO_3.

The reactivity of the samples was generally consistent with the method of impregnation, regardless of the pore structure of the substrate. Samples prepared by the wet impregnation method had the lowest total conversions after 75 min, with total conversions increasing in order of reactive, dry, and in situ impregnation. The dry impregnation method showed varying results from sample to sample, with high conversions for D-48 but lower conversions for D-41 and D-30. This is likely due to the solid-state mixing method, which can be expected to produce materials with a less consistent dispersion of Mo. Importantly, the I-30 sample not only had the highest conversion after 75 min but also retained the largest amount of its initial activity. It is clear that this method produced the most favorable catalyst. This may lead to the use of other acid-prepared mesoporous silicas, such as SBA-3 and SBA-15, as HDS catalysts. SBA-1, another phase produced in acidic solution, has already been shown to be an effective catalyst.[27]

Regeneration. Prior to HDS, samples were off-white due to the presence of MoO_3 in the mesoporous silica. Following catalysis, all materials were brownish-black. The color change is likely due to Mo sulfidation, confirming chemical analysis data. The dark color may also have been due to the presence of residual carbon due to the polymerization of C_4 alkene products from the HDS of thiophene. Calcination in air using the same heating program that was applied following Mo impregnation returned the samples to their original off-white color. Although some decrease in surface areas and pore sizes of samples after catalysis was observed, the physical properties for all materials could be almost completely regenerated by calcination after catalysis. XRD spectra and TEM images of regenerated materials did not show the formation of any Mo clusters. Similarly, the catalytic activity of regenerated materials was almost identical to that of the as-prepared materials. The ability to regenerate these catalysts may make them particularly valuable for HDS applications.

Conclusions

Mesoporous silica doped with Mo has been successfully used as a substrate for the HDS of thiophene. Surface area did not appear to be a significant factor in catalytic performance. When postsynthetic treatments (dry, wet, or reactive impregnation) were used to introduce Mo to the samples, APMS-30 performed significantly better than MCM-41 and moderately better than MCM-48 for this application, regardless of the method of Mo introduction. In situ addition of an Mo source to the APMS-30 synthesis mixture produced a catalyst that retained more of its activity over time than catalysts produced by postsynthetic treatments. The predominance of butane and the presence of a thermodynamic mixture of 2-butenes in the product distribution indicated a mechanism in which initial homolytic cleavage of the thiophene C−S bond and hydrogenolysis to give H_2S and butadiene were followed by rapid hydrogenation to 1-butene, which either underwent slow hydrogenation to butane or was isomerized to a thermodynamic mixture of butenes.

Acknowledgment. This work was funded by the Army Research Office under grant number DAAD19-00-1-0083.

CM030239P

(42) Dhas, N. A.; Ekhtiarzadeh, A.; Suslick, K. S. *J. Am. Chem. Soc.* **2001**, *123*, 8310.
(43) Jayamurthy, M.; Vasudevan, S. *J. Phys. Chem.* **1994**, *98*, 6777.
(44) McMurry, J. *Organic Chemistry*; Brooks/Cole: Pacific Grove, CA, 1996; p 194.
(45) (a) Benson, J. W.; Schrader, G. L.; Angelici, R. J. *J. Mol. Catal. A: Chemical* **1995**, *96*, 283. (b) Luo, S.; Rauchfuss, T. B.; Gan, Z. *J. Am. Chem. Soc.* **1993**, *115*, 4943.